The Cryosphere Discussions

Geophysical evidence for soft bed sliding at Jakobshavn Isbrae, West Greenland

A. E. Block[1,2] **and R. E. Bell**[2]

[1]Department of Earth and Environmental Sciences, Columbia University, New York, New York, 10027, USA
[2]Lamont-Doherty Earth Observatory of Columbia University, Palisades, New York, 10964, USA

Correspondence to: A. E. Block (adrienne@ldeo.columbia.edu)

Title Page

Abstract	Introduction
Conclusions	References
Tables	Figures

|◄ | ►|
◄ | ►

Back | Close

Full Screen / Esc

Printer-friendly Version

Interactive Discussion

Geophysical evidence for soft bed sliding

A. E. Block and R. E. Bell

Abstract

Jakobshavn Isbrae is Greenland's fastest moving outlet glacier and a major contributor to sea level rise. We analyze new gravity and magnetic profiles across the glacier, extending from the mouth of the outlet fjord to 64 km inland of the 2008 grounding line.

5　Our results provide new insights into Jakobshavn Isbrae's geologic underpinnings and controls on the basal velocities. Earlier studies of basal processes minimized basal slip as a fast flow mechanism. Currently, velocities are up to double those considered in these studies, necessitating a reanalysis of the basal conditions. The gravity field along the glacier's main trunk cannot be attributed to the gravitational effect of bed

10　topography and the overlying ice sheet. We interpret the remaining gravity signal as evidence of up to 2400 m of low density sediment beneath the main trunk. Examining recent velocities, we find basal slip is a major contributor to ice flow along most of the sediment filled trough. Within 54 km of the grounding line, only isolated 1–3 km wide regions have velocities that possibly result solely from internal deformation of the

15　ice. We conclude soft bed sliding over the thick sediment wedge beneath Jakobshavn Isbrae is the dominant mechanism of fast flow.

1　Introduction

Jakobshavn Isbrae drains ~7% of the Greenland Ice Sheet (Rignot and Kanagaratnam, 2006) through a ~6 km wide fjord. The seismically detected subglacial trough

20　underlying the main trunk of the glacier is carved into the bedrock but retains some sediment at the bottom (Clarke and Echelmeyer, 1996). The trough, a continuation of the outlet fjord, extends 70 km inland with maximum depths of just over 1500 m below sea level. The main trunk of the glacier is joined by 2 other branches, one from the north that merges near the 2008 grounding line and one from the south, that merges

25　9 km upstream. These branches flow along subdued topographic depressions of 70 m and 30 m respectively. In the main trunk, velocities are more than 1 km yr^{-1} as far as

43 km inland. Near the grounding line, the main trunk of the glacier is moving more than 9 km yr^{-1} while the northern branch is moving just under 5 km yr^{-1}. The southern branch is the slowest moving, with a velocity of less than 1.8 km yr^{-1} where it merges with the main trunk that has a local velocity of ∼6 km yr^{-1} (Joughin et al., 2008).

After the disintegration of a 15 km long floating ice tongue in 1998, the grounding line began retreating (Csatho et al., 2008; Joughin et al., 2008) and the glacier nearly doubled in speed (Joughin et al., 2004). From 2003–2004, the grounding line hovered in the Ice Bay on the south Side of the fjord before stepping further inland to its 2008 location. Since then, the velocity of the glacier's main trunk has increased steadily with marked seasonal speed up in the summer (Joughin et al., 2008). References to the grounding line throughout this work refer to the 2008 location of Csatho et al. (2008).

Here we present new aeromagnetic and gravity data over the Jakobshavn area. We construct models of these data to constrain the regional geologic setting and the geologic control on the observed velocities of Jakobshavn Isbrae. Research in the past 2 decades has shown the trough to be central to understanding the flow of Jakobshavn. Our work examines the role sediments underlying the trough may play in enhancing the glacier's velocity through soft bed sliding. Knowledge of the mechanism(s) of fast flow will contribute a greater understanding of the state and fate of this dynamic glacier.

2 Data

2.1 Gravity acquisition

Airborne geophysical surveys were flown over Jakobshavn Isbrae during June 2008 and as part of NASA's Operation IceBridge (OIB) in May 2010. Transects across the glacier are shown in Fig. 1. The line spacing is usually 5 km. The June 2008 flights were funded by the US National Science Foundation and flown in a De Havilland Company (DHC-6) Twin Otter Aircraft at an average speed of ∼60 m s^{-1} while NASA's 2010 OIB lines were flown at over 160 m s^{-1} in a P-3B aircraft. Both the Twin Otter and OIB flight

operations used the AIRGrav system, owned and operated by Sanders Geophysics Limited. The AirGrav system uses three orthogonal accelerometers oriented relative to an independent three-axis inertial platform that is stabilized with two, two-degrees-of-freedom gyroscopes. Additionally, Schuler tuning controls the platform, ensuring that the gyroscopes and accelerometers are held to within 0.0028° of local level despite motion of the airplane (Studinger et al., 2008).

We have used scalar free-air gravity values filtered at 70 s to analyze subglacial gravity signals from both the Twin Otter and OIB flight lines. Over the inland portion of Jakobshavn, the Twin Otter flight lines are typically 45 km long though over the fjord, these lines are 18–36 km long. There are 4 longer Twin Otter lines that are 130 km in total length extending over 60 km farther north than the majority of the survey lines. The 60 m s^{-1} flight speed results in a gravity full-wavelength resolution of 4.3 km. The OIB flight lines are longer on average, ranging from 71 to 105 km. The OIB P-3B lines have a lower full-wavelength resolution, 11.3 km, due to the faster flight velocity. Many OIB lines are coincident with the Twin Otter lines. In total, there are 17 unique transects that are perpendicular to the glacier's approximate east-west trend inland of the grounding line and 4 unique profiles across the fjord. We have named the lines with a T or B, indicating whether they were flown in the Twin Otter (T) or as part of Operation IceBridge (B), and a number that indicates the approximate km distance from the grounding line. Flight lines down stream of the grounding line are appended with a W as they are west of the grounding line. Because the Twin Otter lines have higher resolution; we show modeled gravity on these lines throughout this work. The longer OIB lines provide additional constraints on the subglacial geology north of the grounding line and along the southern margin of the survey.

2.2 Magnetic field acquisition

The Twin Otter aircraft was equipped with a pod-mounted Scintrex Cesium-3 magnetometer. The total magnetic field was recorded at 10 Hz and subsequently corrected for aircraft motion, diurnal variations and the International Geomagnetic Reference Frame

(IGRF 2008) to obtain regional magnetic anomalies (Fig. 1c). Motion of the airplane creates spurious magnetic signals over a wide range of frequencies that can be removed after a suitable magnetic compensation flight has been flown and magnetic compensation coefficients are calculated. We conducted a magnetic compensation box maneuver at high altitude over a site with low amplitude magnetic anomalies to determine how pitch, roll and yaw motions of the plane impacted the magnetic field observations. Magnetic compensation was determined and removed from magnetic field observations using Pico Envirotec's suite of processing software which was developed after the work of Hardwick (1984). Base station data for Ilulissat, Greenland (station GDH) were obtained from the Geologic Survey of Denmark and Greenland (GEUS). We used these data at 1 Hz to correct for diurnal drift of the magnetic field, limiting the corrected magnetic anomaly grid to ∼3600 m resolution. Finally, to obtain the magnetic anomaly, we removed IGRF 2008 magnetic values for each along track location.

2.3 Radar-derived depths

The Center for the Remote Sensing of Ice Sheets (CReSIS) has collected ice penetrating radar over Jakobshavn since the 1990s. We have used the CReSIS Jakobshavn Glacier Elevation Data which provides ice-bed topography on a 125 m grid (Fig. 1a, https://www.cresis.ku.edu/data/greenland). The grid incorporates radar dating from 1997–2006 as well as ASTER satellite altimetry over exposed rock and Conductivity Temperature Depth (CTD) measurements obtained in the fjord by Holland et al. (2008). The more recent radar data over Jakobshavn was surveyed using a system with a 2 chirp pulse at 150 MHz center frequency as described by Gogineni et al. (2001). Some CReSIS bed elevations have been validated by boreholes drilled to the bed (Luthi et al., 2002) and seismic detection of the subglacial trough (Clarke and Echelmeyer, 1996). CReSIS error estimates are based on the analysis of the crossover points in the radar flights. Preliminary analysis of the crossover residuals suggests the uncertainty of the CReSIS Jakobshavn Glacier Elevation Data is less than 30 m (Joel Plummer, personal communication, 2010).

Geophysical evidence for soft bed sliding

A. E. Block and R. E. Bell

2.4 Surface elevations

NASA's Airborne Topographic Mapper (ATM) surface elevation data based on scanning laser technologies are accurate to approximately 10 cm (Krabill et al., 2002). The ATM system acquired data over the inland portion of Jakobshavn between late June and mid-July 2008, a few weeks after the Twin Otter airborne gravity survey. The ATM laser elevations and ASTER elevations incorporated in the CReSIS grid differ by up to 200 m in exposed rock areas. Subsequently, we have used the ATM data everywhere it is available.

Over the fjord, ATM data has limited spatial coverage. Through a collaboration with the University of Buffalo, we obtained the Jakobshavn digital elevation model created as part of the SPIRIT (Spot Polar Ice: Reference Images and Topographies) project (Bea Csatho, personal communication). These data are obtained through stereoscopic survey by the French Space Agency (CNES). The data has a lateral resolution of 40 m and vertical accuracy of ~5 m (http://polardali.spotimage.fr:8092/IPY/Doc/ SPIRIT_tech_sheet.pdf). Combining high resolution surface elevations with depths to bedrock from CReSIS radar, we are able to constrain ice thickness and surface topography in the survey area at the time the Twin Otter gravity data was acquired.

3 Data description

3.1 Free-air gravity map

The Jakobshavn Free-Air gravity anomaly (Fig. 1b) closely reflects large-scale topographic trends of the CReSIS bed elevation data (Fig. 1a). The values are greatest in the interior (up to + 86 mGal) and decrease to the west (to less than −100 mGal). Superimposed on the regional westward decreasing trend, is a gravity low centered over the trough and fjord. The fjord and trough gravity low, has minimum values of −110 mGal. The trough low begins as a <10 km wide anomaly of approximately

−3 mGal relative to the adjacent bedrock signal at 64 km (T64) from the grounding line. The trough low amplitude increases seaward. The trough low broadens to over 20 km width near the grounding line (between T14 and T0) where it is −75 mGal lower than adjacent bedrock. Over the fjord, 25 km west of the grounding line (T25W), the trough-low anomaly is −60 mGal. Along the fjord, the amplitude of the trough low decreases to −37 mGal near 38 km west of the grounding line (T38W) but increases again to −60 mGal, near the fjord mouth (49W).

3.2 Magnetic anomaly map

The magnetic anomaly map reveals several major features superimposed on the regional magnetic value of −20 nT. The most prominent feature in the magnetic field is a 300+ nT anomaly that trends northeast along the northern margin of the Jakobshavn region. This positive anomaly is 15–50 km wide and is well defined from the fjord mouth to 30 km inland of the grounding line (T49W to T29). The anomaly likely continues to the northeast as it is resolved 49 km inland (T49), however the continuity and width of the anomaly is difficult to resolve due to limited data north of the fjord. The northern branch of Jakobshavn Isbrae parallels the edge of this magnetic high. A 100 nT magnetic low trends northwest over the center of the survey area. This east-west trending anomaly is not as well defined but is spatially coincident with the southern branch of Jakobshavn (T14–T49).

3.3 Definition of gravity residuals

To isolate the component of the free-air signal from the known ice-air and ice-rock interfaces, we forward model the gravity effect of the ice surface and bed elevation along each of the flight lines using GM-SYS. GM-SYS is a profile modeling component of OASIS Montaj that employs 2D potential field methods described by Talwani et al. (1959) and computational algorithms described by Won and Bevis (1987). Gravity models are used to constrain the sediment distribution, fjord depths and the geologic

framework of Jakobshavn. Our initial models include 2 layers of uniform density: glacial ice of 917 kg m^{-3} and bedrock of 2700 kg m^{-3}, consistent with regionally extensive orthogneiss outcropping on the walls both north and south of Jakobshavn's outlet fjord (GEUS, 2009).

Five representative 2-layer forward models between the grounding line and 64 km inland are shown in Fig. 2. The uniform density 2-layer model is assumed to be accurate on a bedrock high on the south side of the fjord. As these points are outside the region of dense crevasses and removed from the major magnetic anomalies, we assume these areas are uniform glacial ice and bedrock. Each profile shows the observed trough-centered gravity low (black dots) and the 2-layer forward modeled gravity (gray line) using the measured ice thickness over a uniform bedrock. The misfits between the simple gravity model and the observed gravity vary systematically. First, the modeled gravity does not recover the amplitude of the trough low on any of the profiles. Secondly, from 20 km inland of the grounding line to the eastern edge of the survey there is a consistent mismatch of ~10 mGal on the northern side of the Jakobshavn trough.

3.3.1 Gravity residual map

To examine the spatial distribution of these gravity differences we have constructed a gravity residual map (Fig. 1d). The residual gravity anomalies are defined by subtracting the 2-layer modeled gravity anomalies from observed free-air anomalies. Under this convention, positive residual values reflect an un-modeled low density body while negative residuals require the addition of a relatively high density body.

Near the grounding line, the trough-centered gravity residuals are between 26 mGal and 28 mGal, the maximum that occurs 19 km inland (T19). Trough residual values gradually decrease inland to <10 mGal. The gravity residual map also emphasizes the contrast between the amplitude and sign of gravity residuals on the north and south sides of Jakobshavn. Immediately south of the trough, gravity residuals are small and rarely have an amplitude greater than 4 mGal. Along the southern margin

Full Screen / Esc

Printer-friendly Version

Interactive Discussion

of the survey, a well defined positive gravity residual of 10 mGal is present between 19 and 39 km inland (B19–B39). This positive gravity residual parallels the trend of the southern branch. north of the glacier, the gravity residuals are positive (up to 36 mGal) and are laterally continuous across the northern-most end of the OIB lines.

5 The maximum amplitude of this broad high occurs 19 km east of the grounding line (T19) with amplitudes decreasing gradually westward toward the mouth of the fjord and more rapidly eastward, toward the interior of the ice sheet. In the west where magnetics are well constrained, the positive gravity residual is spatially coincident with the prominent positive magnetic anomaly.

4   Constraining gravity signals in glaciated regions

Gravity anomalies represent the integration of all densities within a region surrounding the location of data acquisition. We investigated potential sources for the residual gravity anomalies: crevasses, basal till and crustal thickness. We forward modeled the gravity signals resulting from variations in ice density due to crevasses, water storage

15 within the ice, a distributed till layer at the ice sheet base and changes in crustal thickness. The modeling results are summarized in Table 1 and described briefly below. The reported amplitudes assume that the footprint of crevasses or till is as wide as the gravity resolution. Narrower features will have a smaller contribution than reported here.

20 Dense crevasse fields characterize glaciated regions with fast flowing ice. These crevasses may create free space within the glacier body, contributing to negative gravity residuals, or may be filled with water, creating positive gravity residuals. The signal from empty crevasses that penetrate 1 km into the ice sheet and create 10% free space is less than −5 mGal. Water filled crevasses have a smaller amplitude gravity signa-

25 ture because of the small density contrast between water and glacial ice. Water filled crevasses of 1 km depth would contribute only +0.42 mGal to the gravity residual.

Dense crevasses are visible on the surface of Jakobshavn for ∼30 km from the grounding line along the main trunk and the northern and southern glacial branches. At Jakobshavn, the gravity effect from empty crevasses would be a maximum of −5 mGal. Given the amplitude (10–28 mGal) and extent beyond the densely crevassed lower reaches of the glacier, crevassing alone cannot account for the trough-centered residual pattern. As water filled crevasses have a positive gravity signal relative to our 2-layer model, they also cannot resolve the gravity residual pattern. The trough-cenetered gravity residual is not due to the englacial gravity signal of either empty or water-filled crevasses.

Some glaciers have distributed till throughout much of their drainage basins. At Whillans Ice Stream, the seismically detected till is 5–6 m thick but that thickness is spatially variable (Alley et al., 1987). Outside of the Jakobshavn trough, a distributed till layer was modeled with a maximum thickness of 10 m and a variable distribution over the Jakobshavn drainage area. This 10 m thick till contributes less than 1 mGal to the calculated gravity. The signal from a distributed till is too small to be conclusively resolved with these data.

Receiver function analysis has shown that the Proterozoic Greenland land mass is two crustal blocks that are sutured near Jakobshavn Isbrae. To the north, the Moho occurs around 48 km depth, while to the south the Moho transition occurs at 37–42 km (Dahl-Jensen et al., 2003). We forward model potential crustal signals as discrete steps in the Moho. These steps create long wavelength signatures in the modeled gravity anomalies that are not observed in our data. The short wavelength of the north-side residual pattern observed in the Jakobshavn residual map (T19–T49) suggests an origin within the crust for the un-modeled density distribution. Similarly, the 10 km wide trough-centered residual cannot be explained by the proposed step-wise change in crustal thickness. The positive residual seen on the southeastern side of the survey (B19–B39) also is unlikely to be a crustal anomaly due to the wavelength of the residual. The large amplitude (i.e. greater than 5 mGal), short wavelength gravity residuals are not due to variations in crustal thickness but occur within the crust. These residual

anomalies must represent geologically distinct bodies of varying density at or below the ice-rock interface.

5 Gravity interpretation and sediment thickness estimates

5.1 Inland profiles

Along the subglacial trough, we have interpreted the trough-centered positive gravity residual as evidence of low density sediment along the trough. This interpretation is consistent with seismic reflection results that suggest the trough shoulder is bedrock but the center of the trough is lodgement till or compacted sediment (Clarke and Echelmeyer, 1996). We model a sediment body along the trough that will account for the observed residual pattern. Our sediment model focuses on the amplitude of the residual along the main trunk. The assumption of a uniform regional density will result in an upper limit for our sediment depth prediction. After modeling the maximum amount of sediment for our selected density contrast, we will consider the possible sources of other residual signals and their impact on the predicted sediment depth.

The trough-centered gravity residual is modeled as sediment fill with a density of $2130 \, \mathrm{kg \, m^{-3}}$ in a two step, iterative process. First, the sediment is modeled as a polygon that extends straight down from the trough walls to a constant depth. The depth of the sediment polygon is increased until it accounts for the amplitude of the gravity anomaly. Next, the width of the underlying sediment body is decreased until the width of the modeled and calculated gravity anomalies agree. Then, it is often necessary to increase the depth of the sediment polygon to match the observed gravity. The model is accepted when the trough anomaly fits to within 1 mGal. Some representative results of these sediment inclusive models are shown in Fig. 4. There are multiple trade-offs in predicting the geometry of the low density sediment body. First, there is the trade-off between the width and total depth of the low density body. We have modeled the widest low density sediment body that fits the observed gravity. Secondly, there is a trade-off

between overall size of the body and its density contrast with the bedrock. We model sediment at the low end of observed sediment densities, 2130 kg m^{-3}. This approach limits potential overestimation of the sediment thickness in the Jakobshavn trough.

5.1.1 Minimum sediment depth estimates

There are two significant possible error sources in the sediment depth estimates summarized above that would lead to overestimation of the sediment depth: the presence of variable density bedrock adjacent to the trough (between T19 and T49) and extensive crevassing (between T0 and T29). The depth of sediment in our profile models is sensitive to the density contrast with materials on both sides of the trough. The gravity residuals between the broad northern high along the edge of our residual map (on lines B10W to B49) and the trough-centered anomaly are henceforth referred to as the north-side anomaly. As seen in Fig. 1d, the north-side residuals are systematically higher than the south side residuals. This north-side anomaly suggests a relatively low density body may be adjacent to the Jakobshavn trough between 19 and 49 km from the grounding line (T19–T49). If an additional low density body is modeled at the surface next to the sediment, the resulting sediment prediction will be shallower by 10–30%. It is also possible, though not modeled here, that the trough is immediately above a low density body between 19 and 49 km inland (T19–T49). In this case, our minimum estimate for sediment thickness could still be too large.

Gravity anomalies along cross sections of Jakobshavn Isbrae that are within 30 km of the grounding line will be influenced by crevasses (Fig. 1d). Though crevasses cannot explain the entire gravity residual pattern, where present, they will reduce the predicted sediment depth. To obtain a minimum estimate for sediment depth on these lines (T0–T29), we use satellite photos of the region to constrain the lateral extent of dense crevasses and allow these features to create free space in the glacial ice as described in Table 1. It is important to note that near the grounding line (T0–T14) we only observe a trough-centered anomaly. The north-side anomaly is only seen 19 to 49 km from the grounding line (T19–T49). The uncertainty of our estimates of sediment thickness

Title Page

Abstract | Introduction

Conclusions | References

Tables | Figures

⏮ | ⏭

◀ | ▶

Back | Close

Full Screen / Esc

Printer-friendly Version

Interactive Discussion

near the grounding line (T0–T14) are not influenced by the north-side anomaly and only depend on gravity signals from crevasses, which have a maximum amplitude of 5 mGal. This leaves a 21–23 mGal positive gravity residual that is attributed to thick sediments beneath the trough.

5.2 Fjord profiles

Although interior profiles are constrained by radar, bathymetric measurements in the fjord are sporadic. Holland et al. (2008) collected point depth measurements in the fjord that indicate depths of 741 to 826 m with an average depth of 785 m. Using the CReSIS elevations, the forward model 10 km west of the 2008 grounding line (T10W) shows a positive gravity residual suggesting sediment fill continues into the fjord. Thus the additional fjord profiles each have two unknowns, depth of the fjord and sediment fill in the fjord.

To estimate the thickness of fjord fill sediment, we must first constrain the depth of the fjord. None of the Holland et al. (2008) points are in the center of the fjord and thus may underestimate its maximum depth. To estimate depth in the fjord, we have assumed it is roughly parabolic, like the interior trough (T54 to T19) and that the exposed walls are representative of the slope of the fjord walls below sea level. If these two assumptions are in conflict, we allow observed fjord wall slopes to dominate the prediction. This assumption is validated by the fjord shape detected by radar 10 km west of the grounding line (T10W) where the fjord wall slope continues below sea level (Fig. 3). Fjord fill is modeled at a constant density of 1010 kg m^{-3} consistent with sea water. These assumptions result in fjord depth predictions slightly deeper than the CTD maximum of 826 m. The synthetic fjord profiles yield a fjord depth that is nearly flat with maximum depths of 851 m at 25 km west of the grounding line (T25W), 898 m at 38 km west (T38W) and 800 m at the fjord mouth (T49W). The predicted fjord geometry suggests that gravity residuals in the fjord are relatively constant, at ~14 mGal from 25 km west of the grounding line to the fjord mouth (T25W to T49W). We model sediments in the fjord from these gravity residuals as previously described

for the inland profiles (Sect. 5.1). An example is shown in Fig. 4 and other sediment thickness estimates are summarized below.

5.3 Sediment description

Based on our gravity modeling we can present an along axis profile of the sediment depths along Jakobshavn's main trunk (Fig. 5).This profile follows the center-line of the subglacial trough (Labeled AXIS, Fig. 1). In this description, we highlight minimum sediment thicknesses and their corresponding depths. These estimates assume that the bed elevations in the CReSIS grid are accurate. Given the 30 m crossover error, there could be ±100 m of additional sediment. In the fjord, we estimate our predicted depths are within ∼100 m of true fjord depths, resulting in sediment depth uncertainties of ±300 m.

On our most inland profile, 64 km east of the grounding line (T64), we predict sediments of ∼300 m thickness. The sediments pinch out completely between 59 km and 54 km inland. The sediments then thicken to 400 m and reach more than 2 km depth by 49 km from the grounding line (T49). Further downstream, the sediments continue to thicken to 2400 m, reaching depths of 3200 m below seal level at 14 km inland (T14). At the grounding line, we predict sediments are 1 km thick. In the fjord (T10W to T38W), the sediments are a nearly uniform depth of 2200 m, corresponding to a thickness of approximately 1400 m. After accounting for the narrowing of the fjord, sediments at the fjord mouth may be up to 1900 m thick, extending to between 2700 m to 3200 m below sea level.

6 Discussion

Using gravity and magnetics we have documented the geological framework of Jakobshavn Isbrae and identified a thick sediment sequence at the base of its subglacial trough. The sediment thickness is up to 2400 m and appears to pinch out

~54 km upstream of the 2008 grounding line, 100 km from the fjord mouth. This finding is consistent with analysis of seismic reflection coefficients which suggest the trough is cut into bedrock while the center line is underlain by lodgement till and/or sediments within the density range of 2000–2500 kg m^{-3} (Clarke and Echelmeyer, 1996). Here we consider the origin of the sediment filled trough and discuss the role the sediments play in the evolution of Jakobshavn Isbrae.

Basal sediments are known to lubricate ice flow and can trigger the onset of ice streaming but have not been considered to be important beneath Greenland outlet glaciers. In Antarctica, the presence of sedimentary basins has been associated with the onset of fast flow both in the Ross ice streams (Anadakrishnan et al., 1998; Bell et al., 1998; Studinger et al., 2001) and in the drainage to the Weddell Sea (Bamber et al., 2006). These sedimentary basins provide the necessary material to support till lubricated sliding. Observations of basal till at Whillans Ice Stream (formerly Ice Stream B) suggest till deformation begins at 3–8 kPa, a value less than one tenth of that for internal ice deformation (Alley et al., 1987). Near the grounding line, an unfrozen, saturated till dictates the motion of the glacier through basal slip. Although the seismically detected till layer is 9 m thick, only the upper 3 cm are deforming and contributing to basal slip (Engelhardt and Kamb, 1998). Deformable till, even in small quantities, can contribute to basal slip and increase a glacier's velocity from the onset of flow to the grounding line.

In contrast to the West Antarctic Ice Streams, there is no evidence from coastal outcrops that Jakobshavn Isbrae occupies a tectonically-derived, sedimentary basin. The predicted depth to the base of the sediments shows local over-deepenings, consistent with a glacially carved trough. Although set in a Proterozoic basement, the trough is sediment filled as the result of the deposition of glacial material over the past 2.7 MY as the Greenland ice sheet waxed and waned. This material may include sediments, glacial lake infill and marine sedimentation. We also consider the sediments to be wet because the entire trough is below sea level and connected to the outlet fjord. Also borehole temperatures in basal ice are at the melting point (Luthi et al., 2002)

suggesting that englacial water could reach the bed. The presence of sediments is not sufficient evidence of soft bed sliding as a mechanism of fast flow at Jakobshavn Isbrae. We will now couple our sediment finding to an argument for high rates of basal slip.

Based on data collected between 1986–1989, many studies (Funk et al., 1994; Iken et al., 1993; Luthi et al., 2002) have addressed the mechanism(s) of fast flow along the glacier's main trunk and near the grounding line. Despite the suggestion of till at the center line (Clarke and Echelmeyer, 1996), these studies repeatedly find that basal sliding is relatively unimportant along Jakobshavn's flow line (Clarke and Echelmeyer, 1996; Luthi et al., 2002). The velocity of the glacier has been attributed to the trough itself because its geometry concentrates geothermal heat, contributing to warm englacial temperatures. This warmth increases the thickness of highly deformable temperate ice at the base of the glacier (Iken et al., 1993). Funk et al. (1994) show internal deformation of the ice accounts for up to 60% of the velocity of the glacier even at distances of 45 km from the grounding line. In contrast, Luthi et al. (2002) observe a location where 60% of the velocity of the glacier is due to basal motion. They ascribe the large basal sliding contribution to unique circumstances on the shear margin on the side of the ice stream and do not consider it representative of flow mechanisms along the main trunk.

Clarke and Echelmeyer (1996) argued that the basal shear stress required to account for the velocity of Jakobshavn could be produced by internal deformation of an ice sheet between $-3\,^{\circ}$C and $-8\,^{\circ}$C. They consider the magnitude of two shear stress terms. T_{o} is the shear stress needed to account for the observed surface velocities based on the assumption that internal deformation is the only mechanism of flow. T_{b} is basal shear created by the glacier's surface slope which drives the internal deformation of the ice. If the shear stress necessary to account for observed velocities is greater than the shear stress provided by the surface slope ($T_{o} > T_{b}$), than basal slip is important or the assumed temperature of the ice sheet is too cold.

Geophysical evidence for soft bed sliding

A. E. Block and R. E. Bell

Title Page

Abstract | Introduction

Conclusions | References

Tables | Figures

◄◄ | ►►

◄ | ►

Back | Close

Full Screen / Esc

Printer-friendly Version

Interactive Discussion

The shear stress required to drive an observed ice velocity, u_o is given by

$$T_o = \left(\frac{2u_o}{AH} \right)^{\frac{1}{3}} \tag{1}$$

where A is the temperature dependent flow-law parameter, H is the ice thickness and the flow law exponent is assumed to be 3.

At Jakobshavn, the basal shear, T_b, is calculated in the traditional way with the addition of a shape factor for the trough at each cross section:

$$T_b = F\rho gH\sin(\alpha) \tag{2}$$

Where F is the shape factor (values between 0 and 1), ρ is the density of ice, g is the acceleration due to gravity, H is ice thickness and α is average surface slope. Methods for estimating the shape factor of the trough include the approach from Nye (1965) which provides a minimum shape factor, a definition derived by Clark and Echelmeyer (1996) which provides a maximum shape factor and interpolation from the data presented by Cuffey and Patterson (2010) which includes shape factors for both parabolic and ellipsoidal shapes.

Based on velocity observations from 1986, Clarke and Echelmeyer calculated T_o and T_b values for shear stress at 4 locations along the trough between 6–60 km inland of the current grounding line and find that basal sliding was not clearly important at any of them. At their fastest moving survey location, Jakobshavn's velocity was 3.8 km yr^{-1}. In the time since analysis of the 1986–1989 data resulted in the conclusion that basal slip is not important at Jakobshavn Isbrae (Clarke and Echelmeyer, 1996; Luthi et al., 2002), the velocity of the glacier has increased, nearly doubling at the grounding line (Joughin, 2008).

In light of our interpretation of sediment fill at the base of the radar-detected trough and the increased surface velocity of Jakobshavn from Joughin et al. (2008), we have revisited the basal stress analysis of Clarke and Echelmeyer (1996) with 3 updates. (1) We have used a velocity grid that provides the average surface velocity for Fall

2000 (Joughin et al., 2008). (2) We have used the values reported by Cuffey and Paterson (2010) to calculate shape factor for the trough at each crossing and linearly interpolate values in between each calculation. In doing so, we treat all of the interior profiles as parabolas while using ellipse shape factor values near the trough onset and at the grounding line to reflect the broadened expression of the trough in those locations (as shown in Fig. 2). (3) Because boreholes to the base of Jakobshavn show the basal temperature to be $-0.6\,°$C (Luthi et al., 2002) we consider average temperatures between $-3\,°$C and $0\,°$C to eliminate false positives for basal sliding. The results of this analysis are shown in Fig. 6.

Along most of the trough mid-line, $\sim$40 km of the 64 km grounded portion, the value of T_o needed to explain modern velocities is larger than the shear stress provided by the surface slope. We propose that basal sliding dominates the velocity of the lower $\sim$50 km of Jakobshavn Isbrae. Regions where internal deformation of the glacier could explain the observed velocities are shaded gray and referred to as no-slip-required (NSR) regions. This nomenclature emphasizes that slip is not required to explain the surface velocity, however these regions could be slipping. The ice just inland of the grounding line of Jakobshavn Isbrae is a NSR region. The surface slope is steep enough to account for the observed 9+ km yr^{-1} (Joughin et al., 2008). Between 50–100 km from the fjord mouth, there are isolated NSR stretches spanning 1–3 km of the glacier. These NSR locations are coincident with local steepening of the ice surface and frequently bumps in the basal topography. There are broader NSR regions beginning at 107 km from the fjord mouth. At 110 km, the NSR region is coincident with the location where the sediments in the trough pinch out. Our results strongly suggest that basal slip is an important component of motion along the majority of Jakobshavn Isbrae and that basal slip is restricted to where the subglacial trough is filled with sediment.

A. E. Block and R. E. Bell

Title Page

Abstract | Introduction

Conclusions | References

Tables | Figures

◄ | ►

◄ | ►

Back | Close

Full Screen / Esc

Printer-friendly Version

Interactive Discussion

7   Conclusions

The subsurface geology of Jakobshavn Isbrae is more diverse than coastal outcrops would suggest and may impact all 3 glacial branches. The main trunk of the glacier is characterized by a positive gravity residual, indicating low density material exists within the trough. We attribute this anomaly to a sediment wedge of up to 2400 m thickness that reaches more than 54 km inland of the grounding line. The sediments fill a glacially carved over-deepening that has formed and filled in response to fluctuations of the Greenland Ice Sheet since 2.7 MA. The northern branch of Jakobshavn is parallel to the edge of a magnetic high of more than 300 nT while the southern branch parallels a positive gravity residual and lies within a magnetic low. This suggests that the location of the smaller glacier branches may be geologically controlled.

Along most of the main trunk, the observed surface velocity of Jakobshavn Isbrae is not due solely to internal deformation of the ice and basal slip must occur. However, there are some regions along the glacier where slip is not required to explain observed velocities. These include isolated stretches of 1–3 km beginning just inland of the grounding line and a 5+ km stretch at 54 km from the grounding line where the predicted sedimentary wedge pinches out. Basal slip is only necessary to explain the velocity of the glacier in places where there are sediments at the base, providing a weak, deformable bed. A total of 40 km of the 64 km inland portion of Jakobshavn requires basal slip to attain the observed velocities. We conclude that soft bed sliding is the dominant mechanism of fast flow at Jakobshavn Isbrae.

References

Alley, R., Blankenship, D. D., Bentley, C. R., and Rooney, T.: Till beneath Ice Stream B 3. Till Deformation: Evidence and Implications, J. Geophys. Res., 92(B9), 8921–8929, 1987.

Anandikrishnan, S., Blankenship, D. D., Alley, R. B., and Stoffa, P. L.: Influence of subglacial geology on the position of a West antarctic ice stream from seismic observations, Nature, 394, 62–65, 1998.

Bamber, J. L., Ferraccioli, F., Joughin, I., Shepherd, T., Rippin, D. M., Siegert, M., and Vaughan, D. G.: East Antarctic ice stream tributary underlain by major sedimentary basin, Geology, 34(1), 33–36, 2006.

Bell, R. E., Blankenship, D. D., Finn, C. A., Morse, D. L., Scambos, T. A., and Hodge, S. M.: Influence of subglacial geology on the onset of a West Antarctic ice stream from aerogeophysical observations, Nature, 394, 58–62, 1998.

Clarke, T. S. and Echelmeyer, K.: Seismic Reflection evidence for a deep subglacial trough beneath Jakobshavns Isbrae, West Greenland, J. Glaciol., 43(141), 219–232, 1996.

Csatho, B., Schenk, T., Van Der Veen, C. J., and Krabill, W. B.: Intermittent thinning of Jakobshavn Isbrae, West Greenland, since the Little Ice Age, J. Glaciol., 54(184), 131–144, 2008.

Cuffey, K. M. and Paterson W. S. B.: The Physics of Glaciers, 4th Edn., Butterworth-Heinemann of Elsevier, Burlington, MA, USA, 693pp, 2010.

Dahl-Jensen, T., Larsen, T., Woelbern, I., Bach, T., Hanka, W., Kind, R., Gregersen, S., Mosegaard, K., Voss, P., and Gudmundsson, O.: Depth to Moho in Greenland: receiver function analysis suggests two Proterozoic blocks in Greenland, Earth Planet Sc. Lett., 205, 379–393, 2003.

Funk, M., Echelmeyer, K., and Iken, A.: Mechanisms of fast flow in Jakobshavns Isbrae, West Greenland: Part II: Modeling of englacial temperatures, J. Glaciol., 40(136), 569–585, 1994.

Geological Survey of Denmark and Greenland (GEUS): En foldet udgave af kortet er inkluderet i publikationen: Greenland from Archaean to Quaterny, Geology Survey of Denmark and Greenland Bulletin 18, http://www.geus.dk/geuspage-uk.htm, 2009.

Gogineni, S., Tammana, D., Braaten, D., Leuschen, T., Akins, T., Legarsky, J., Kanagaratnam, P., Stiles, J., Allen, C., and Jezek, K.: Coherent radar ice thickness measurement over the Greenland ice sheet, J. Geophys. Res., 16(D24), 33761–33772, 2001.

Hardwick, C. D.: Non-oriented cesium sensors for airborne magnetometry and gradiometry, Geophysics, 49(11), 2024–2031, 1984.

Holland, D. M., Thomas, R. H., De Young, B., Ribergaard, M. H., and Lyberth, B.: Acceleration of Jakobshavn Isbrae triggered by warm subsurface ocean waters, Nat. Geosci., 1, 659–664, 2008.

Iken, A., Echelmeyer, K., Harrison, W., and Funk, M.,: Mechanisms of fast flow in Jakobshavns Isbrae, West Greenland: Part I: Measurement of temperature and water level in deep boreholes, J. Glaciol., 39(131), 15–25, 1993.

Joughin, I., Abdalati, W., and Fahnestock., M.: Large Fluctuations in speed on Greenland's

Jakobshavn Isbrae glacier, Nature, 432, 608–610, 2004.

Joughin, I., Howat, I. M., Fahnestock, M., Smith, B., Krabill, W., Alley, R. B., Stern, H., and Truffer M.:Continued evolution of Jakobshavn Isbrae following its rapid speedup, J. Geophys. Res., F04006, 113, doi:10.1029/2008JF001023, 2008.

Krabill, W. B., Abdalati, W., Frederick, E. B., Manizade, S. S., Martin, C. F., Sonntag, J. G., Swift, R. N., Thomas, R. H., and Yungel, Y. G.: Aircraft laser altimetry measurement of elevation changes of the Greenland ice sheet: technique and accuracy assessment, J. Geodyn., 34, 357–376, 2002.

Luthi, M., Funk, M., Iken, A., Gogineni, S., Truffer, M.: Mechanisms of fast flow in Jakobshavns Isbrae, West Greenland: Part III: Measurement of Ice deformation, temperature and cross-borehole conductivity in boreholes to the bedrock, J. Glaciol., 48(162), 369–385, 2002.

Nye, J. F.: The flow of a glacier in a channel of rectangular, elliptic or parabolic cross-section, J. Glaciol., 5(41), 661–690, 1965.

Rignot, E. and Kanagaratnam, P.: Changes in the velocity structure of the Greenland Ice Sheet, Science, 311(5763), 986–990, 2006.

Studinger, M., Bell, R. E., Blankenship, D. D., Finn, C., Arko, R. A., Morse, D. L., and Joughin, I.: Subglacial Sediments: A Regional Geological Template for Ice Flow in West Antarctica, Geophys. Res. Lett., 28(18), 3493–3496, 2001.

Studinger, M., Bell, E., and Frearson, N.: Comparison of AIRGrav and GT-1A airborne gravimenteres for research applications, Geophysics, 73(6), I51–I61, 2008.

Talwani, M., Worzel, J. L., and Landisman, M.: Rapid Gravity Computations for Two-Dimensional Bodies with Application to the Mendocino Submarine Fracture Zone, J Geophys. Res., 64(1), 49–59, 1959.

Won, I. J. and Bevis, M.: Computing the gravitational and magnetic anomalies due to a polygon: Algorithms and Fortran subroutines, Geophysics, 52, x0.2, 232–238, 1987.

A. E. Block and R. E. Bell

Table 1. Other gravity Signals in glaciated regions. Maximum amplitudes are for Jakobshavn specifically based on assumptions described in the comments section.

Signal origin	Gravity Signal Per 10 m	Maximum amplitude	Comments
Ice surface elevation error	0.38 mGal	76 mGal < 0.038 mGal	Regional DEM differs from laser by 200 m. 10 cm uncertainty in ATM elevations.
Bed-ice elevation error	0.75 m Gal	2.241 mGal	Based on 30 m uncertainty of CReSIS bed elevation data.
Rock surface elevation error	1.13 mGal	0.57 mGal	Based on 5 m uncertainty of SPOT elevations over the fjord.
Distributed till (i.e. sediment in place of bedrock)	0.24 mGal	0.24 mGal	A distributed till of maximum 10 m thickness. Densities as in Fig. 2.
Crevasse- empty	0.38 mGal	−3.8 mGal	Crevasses create an average of 10% free space to a depth of 1 km.
Crevasse- water filled	0.042 mGal	+0.42 mGal	Crevasses filled with 10% water to depth of 1 km.
Moho		35 mGal	Allow 2 km crustal thickness change to Moho of 3300 kg m^{-3}. Even as a Moho step, crustal thickness changes impose long wavelength trend in gravity data beyond the wavelength of these data.

Full Screen / Esc

Printer-friendly Version

Interactive Discussion
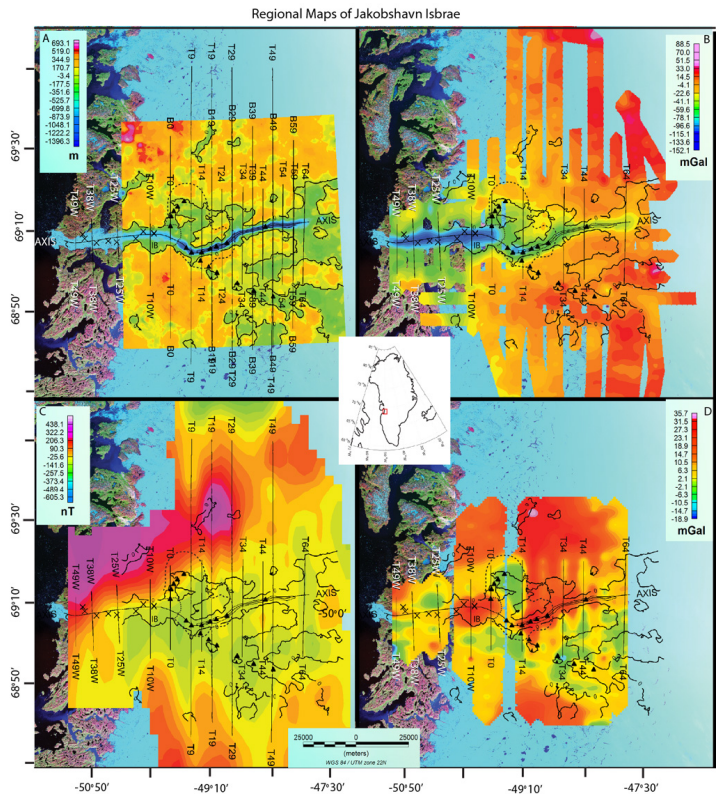
Fig. 1. Jakobshavn regional maps. The 2008 grounding line is stippled. The region of dense crevassing as identified from LANDSAT imagery is surrounded by a dashed line. IB-Ice Bay. **(A)** CReSIS's Jakobshavn Glacier Data. **(B)** Free Air Gravity Anomalies. **(C)** Magnetic Data gridded at 3600 m. **(D)** Gravity Residuals (see text for definition). Profiles from NASA's Operation IceBridge (B) and the Twin Otter based (T) airborne surveys are shown. Profiles are named for flight type (B or T) and by approximate distance from the 2008 grounding line. Triangles indicate locations of Joughin et al. (2008) velocity observations. X's show the locations of fjord depth from CTD by Holland et al. (2008).
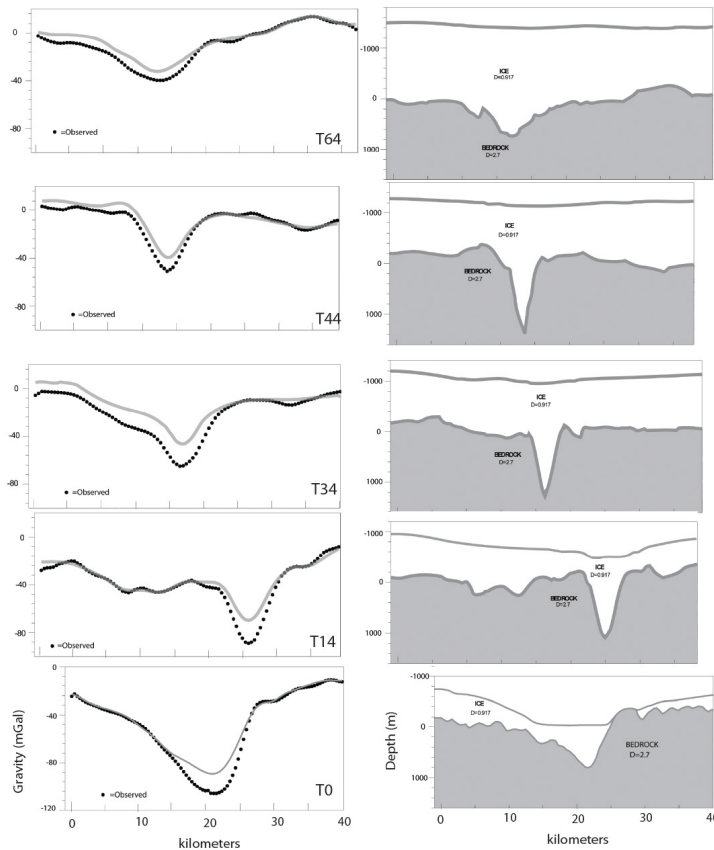
Fig. 2. Inland Profiles across Jakobshavn Isbrae. Observed and calculated gravity anomalies are shown on the left. The calculated gravity assumes a uniform 2-layer model. Densities are indicated in g cm^{-3}. The north-side of the trough shows a positive gravity residual on T34, T44 and T64. Horizontal offset of the models is intentional and reflects the geographic position of the survey lines.
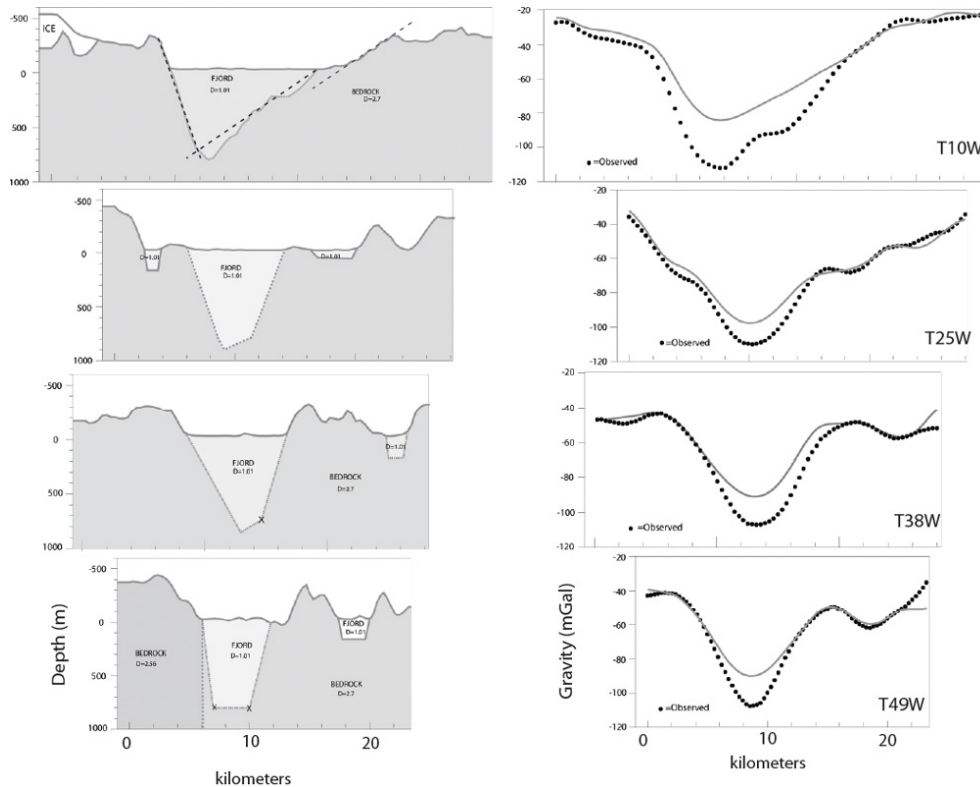
Fig. 3. Fjord gravity observations, geometry predictions and gravity residuals. Densities are indicated in $g\,cm^{-3}$. Fjord depth is estimated using slope on the fjord side walls and nearest Holland et al. (2008) CTD depths. T10W shows the justification of the method. The slope of the side walls is shown in dashed lines and moved to the fjord edges (dashed lines) to illustrate the fjord geometry we would predict along that line. Other profiles are similarly predicted. The closest Holland depth point is incorporated into the model where indicated by an X. Estimated gravity residuals for each profile are shown on the right.
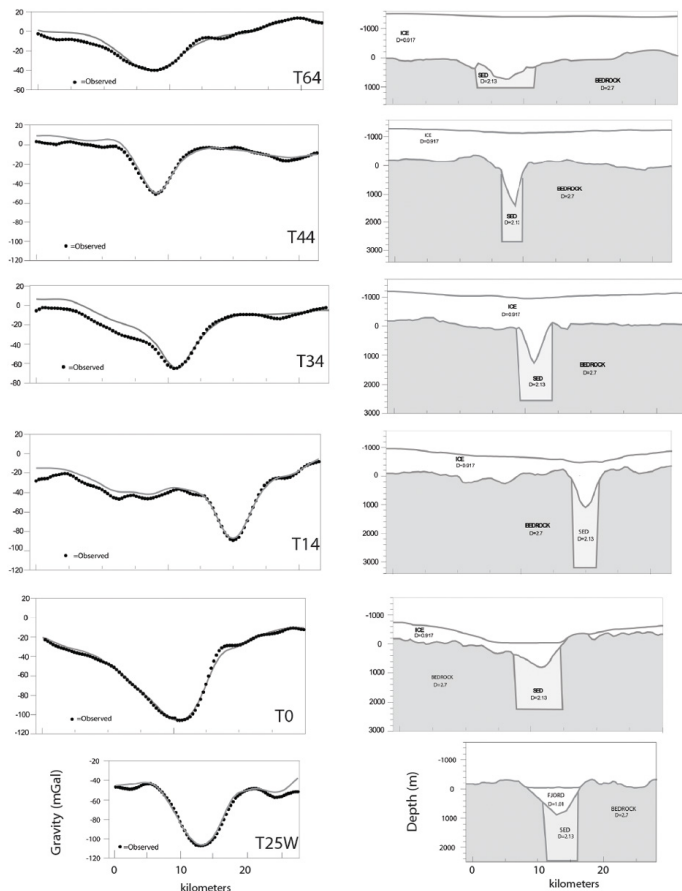
Fig. 4. Prediction of maximum sediment thickness from observed gravity residuals for inland profiles from Fig. 2 and one additional fjord profile (T25W). Sediment is thickest between 19 km and 14 km (T14) from the grounding line. Thickness at the grounding line (T0) is 1 km, comparable to the 1400 m predicted in the fjord. At the fjord mouth and near the grounding line, the sediment-filled trough is over-deepened.

Title Page

Abstract | Introduction

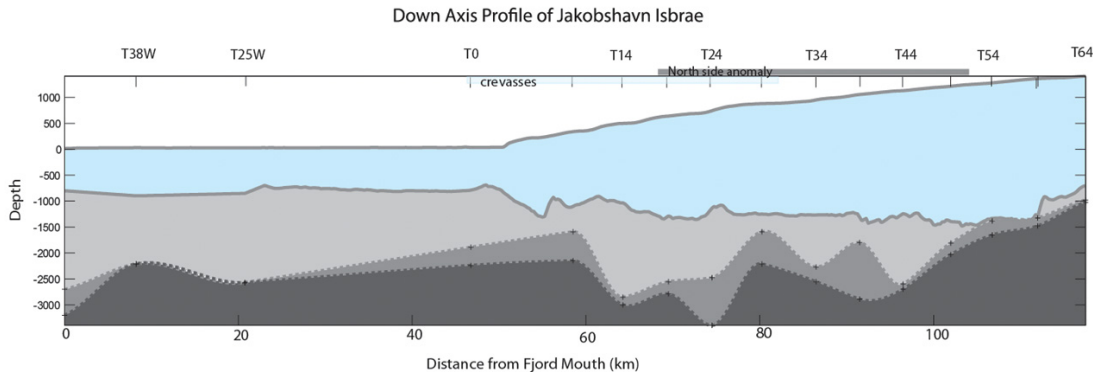Conclusions | References

Tables | Figures
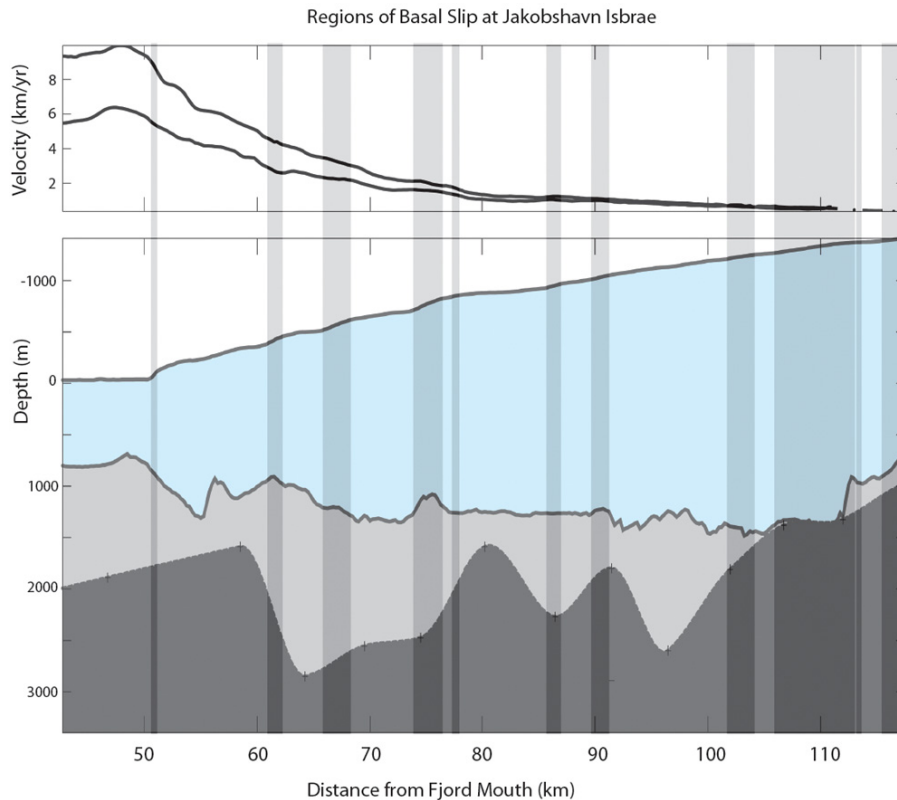
◄ | ►

◄ | ►

Back | Close

Full Screen / Esc

Printer-friendly Version

Interactive Discussion

Fig. 5. Down Axis Profile of Jakobshavn Isbrae (AXIS in Fig. 1) showing predicted sediment thickness minimum and maximum. The ice and fjord fill are shown in blue, sediments in gray (2 shades) and bedrock in a dark gray. Gray interfaces are, from top to bottom, the ATM ice surface, CReSIS ice base, minimum sediment depth estimate (dashed) and maximum sediment depth estimate (dashed). Sediment curves are Akima interpolated with control points as marked with crosses. The horizontal scale at the top shows the corresponding control cross sections. Also shown along the top axis are bars indicating where other gravity signals influence the sediment estimate. The blue bar indicates crevasses are present and the gray bar shows where there is a trough adjacent low density body.

Title Page

Abstract | Introduction

Conclusions | References

Tables | Figures

◄◄ | ►►

◄ | ►

Back | Close

Full Screen / Esc

Printer-friendly Version

Interactive Discussion

Regions of Basal Slip at Jakobshavn Isbrae

Fig. 6. Predicted soft bed sliding at Jakobshavn Isbrae. Regions that do not require slip (NSR) are shown with gray shaded vertical bars. Lower panel: Cross section of Jakobshavn inland of the grounding line (as in Fig. 5, only minimum sediment estimate is shown). Top panel: Velocity observations from 1992, 1994–1995 that pre-date the speed up (Joughin et al., 2004) and from Fall 2000 (Joughin et al., 2008).